8 Medical Imaging

8-1 X-Ray Phase Imaging/ Tomography Using Talbot Interferometry

In the field of synchrotron radiation imaging, various phase-contrast methods have been proposed and demonstrated since the early 1990's, aiming at improving sensitivity to weakly absorbing materials such as soft matter and biological objects. Three-dimensional imaging (phase tomography) based on these methods has also been achieved.

The X-ray Talbot interferometer [1-3], a comparatively new device for phase-contrast imaging, consists of two transmission gratings positioned along the optical axis between the sample and the image detector, as shown in Fig. 1. This simple optical configuration generates a differential phase contrast. Outstanding advantages of Talbot interferometry are: (a) polychromatic radiation can be used, and (b) the cone-shaped beam is available and provides a large field of view. Talbot interferometry is therefore a valuable approach for synchrotron radiation phase-sensitive imaging. In addition, it is also expected that the technology will mature in the future from the current exploratory experiments into a practical X-ray phase imaging method not relying on a synchrotron facility.

The principle of Talbot interferometry is as follows: (1) A phase grating under coherent illumination forms a periodic intensity pattern by the Talbot effect at a specific distance downstream. This intensity pattern has a pitch corresponding to that of the phase grating, and is therefore called a self-image. (2) When an object is placed in front of the phase grating, the self-image is deformed due to refraction at the object. (3) An amplitude grating which has a pitch almost equal to that of the self-image is placed at the position of the self-image. Moiré fringes are generated by the superposition of the deformed self-image and the pattern of the amplitude grating. In general, the spacing of the moiré fringes is much larger than the grating pitch, and can easily be resolved using a normal X-ray image detector. Differential phase information can be obtained from the deformation of the moiré fringes. For quantitative measurements, the fringe scanning method can be used by displacing one of the gratings in the direction of its diffraction vector. By repeating the measurement at various sample rotations, tomographic image reconstruction is attained.

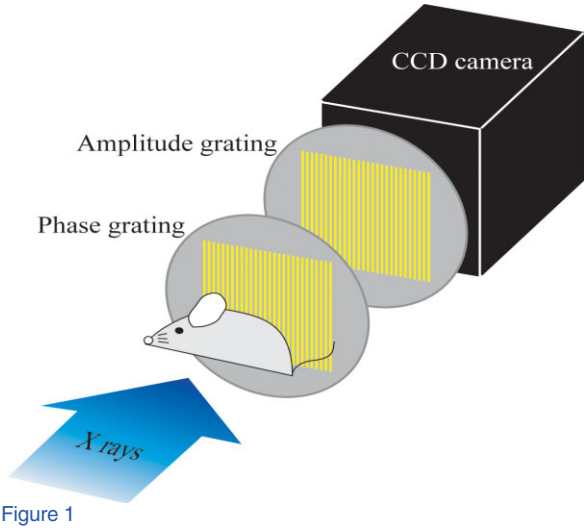

Figure 1
Setup for the Talbot interferometer X-ray phase imaging technique, showing the two gratings.

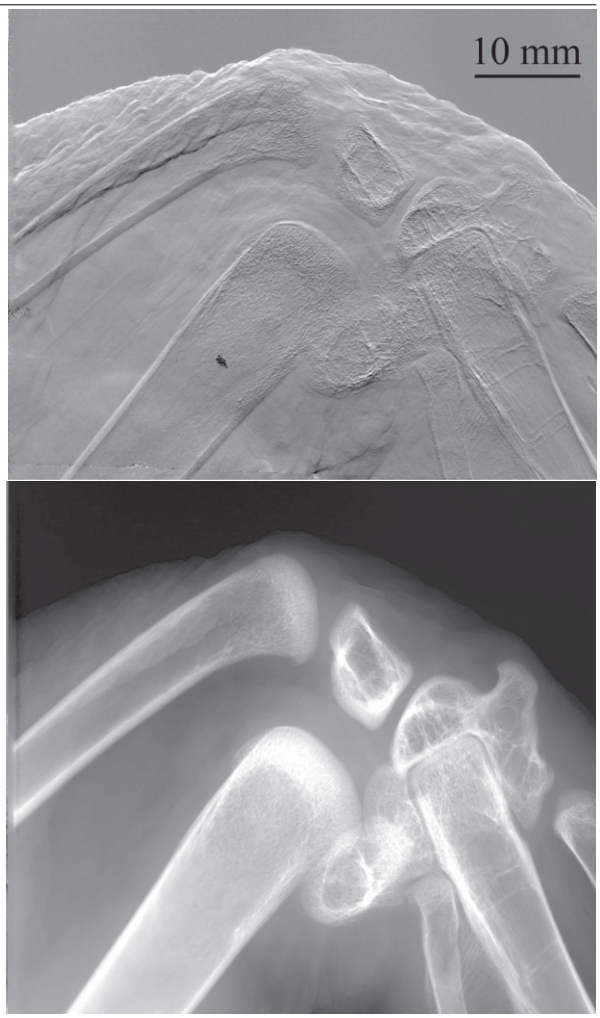

Figure 2
Differential phase image (top) and absorption image (bottom) obtained for a chicken wing joint.

Figure 2 shows a differential phase image of a chicken wing joint obtained using the fringe scanning method with 27.6-keV X-rays at BL-14C1. In this experiment, phase and amplitude gratings with 5.3 μm pitch and 60 mm × 60 mm area were used. The X-ray beam section, generated with an asymmetric crystal, determined the actual image size (28 mm × 22 mm), which was

recorded using a CCD-based image detector (4k × 4k pixels) with an effective pixel size of 18 μm. The amplitude grating, which needs a high aspect-ratio structure, was fabricated using X-ray lithography at NewSUBARU, Japan, and by gold electroplating, in collaboration with University of Hyogo (Prof. T. Hattori).

The X-ray Talbot interferometer functions with a white beam and filters, enabling phase imaging with a short exposure. Next, we plan to pioneer high-speed X-ray phase imaging, taking advantage of the distinctive feature.

A. Momose (The Univ. of Tokyo)

References

[1] A. Momose, S. Kawamoto, I. Koyama, Y. Hamaishi, K. Takai and Y. Suzuki, *Jpn. J. Appl. Phys.*, **42** (2003) L866.
[2] T. Weitkamp, B. Nöhammer, A. Diaz, C. David and E. Ziegler, *Appl. Phys. Lett.*, **86** (2005) 054101.
[3] A. Momose, W. Yashiro, Y. Takeda, Y. Suzuki and T. Hattori, *Jpn. J. Appl. Phys.*, **45** (2006) 5254.

8-2 Elucidation of Microvascular Response Using Synchrotron Radiation Micro-Angiography

We plan to establish synchrotron radiation micro-angiography (SR-MA) in order to investigate various physiological and pathological responses of microvasculature to external and internal stimuli. These responses can only be visualized using SR-MA. We describe here briefly some new results obtained from research at AR-NE5A.

The SR-MA technique makes use of an asymmetrically cut silicon crystal to vertically expand the monochromatic beam, a fluorescent screen, a CCD camera (Model C4880, Hamamatsu Photonics), and a computer data storage system. The system is used to record two-dimensional images with a spatial resolution of 26 μm, and the visual field is 26 mm × 26 mm. Exposure times range from 30 ms to 5 s, with a maximum acquisition rate of 3 images/s. Inorganic iodine with an iodine concentration of 32% by weight is used as the contrast material. With the SR-MA technique vessels down to 50 μm in diameter were identified under static conditions, and down to 100 μm in the beating heart (Figs. 3, 4).

1. Smoking and acute peripheral vascular response

Smoking is a potential risk to human health, being linked to problems such as vascular disease. Although it is known that smoking brings about vascular constriction in general, the details have not been investigated. From our experiments, we can conclude that smoking causes vascular constriction (down to 63%) only in vessels larger than 100 μm in diameter, coinciding with the action of NO donors [1].

2. Response to cold of deep arteries in lower extremities

Cold temperatures are also thought to bring about vascular constriction. However, the visualization of vessels under exposure to cold has not previously been investigated. From our observations, deep arteries of the extremities appear to enlarge under coldness, rather than constrict. The response is so fast that vascular expansion starts within 2-3 s following exposure to cold. It was also observed that exposure to cold of one lower extremity also induces prompt expansion in the unexposed lower extremity.

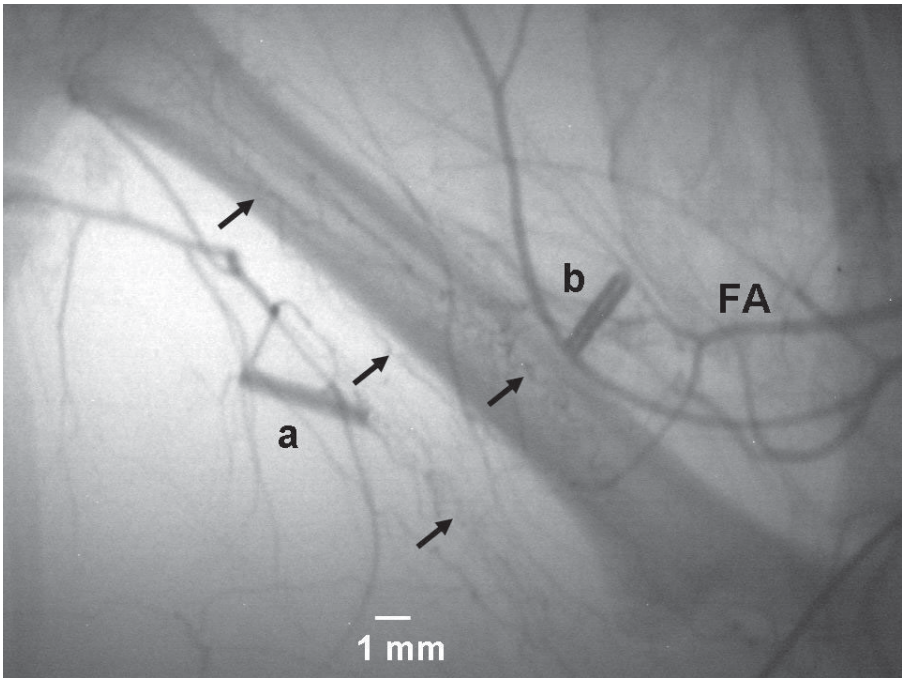

Figure 3
SR-MA of lower rat limb 4 weeks after an operation to ligate and resect the femoral artery (marked FA) between clips “a” and “b”. Spiral-shaped collateral formation (arteriogenesis) is revealed (arrows). Newly-formed vessels of sizes down to 50 μm are identified.

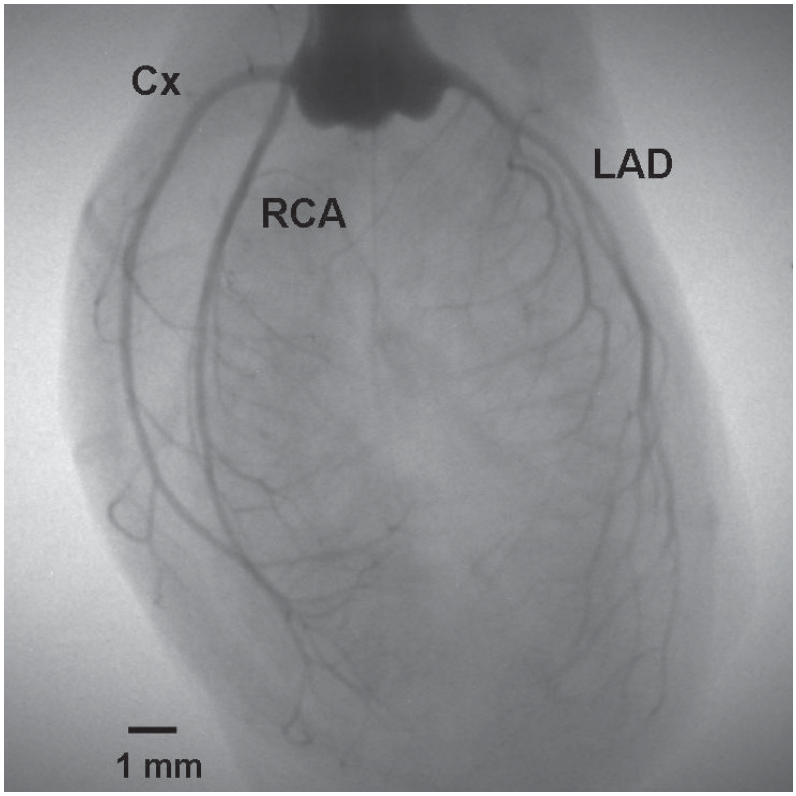

Figure 4
SR-MA of rat coronary arteries. Three major coronary arteries (LAD, Cx, RCA) and their 2nd branches are revealed. The minimum diameter of the identified vessels is 50 μm. This method was successfully used to investigate coronary spasms and vascular regeneration.

3. Gender difference against cold exposure

It turns out that there is a gender difference in the rate of expansion following cold exposure, with male rats showing larger expansions than female rats. Ovariectomized female rats were intermediate between the two extremes. These findings may explain why females (especially young women) are more sensitive to cold.

4. Coronary vascular spasm

Coronary angiography using excited rat hearts in a Langendorff apparatus can be used to identify vessels down to 100 μm in the beating heart [2]. Coronary spasms were induced using a voltage-gated potassium channel blocker (Kv channel blocker), which has not been shown previously. With the higher spatial resolution of the current technique, microvascular spasms can be visualised, which was impossible using conventional X-ray systems due to technical limitations. Females are more sensitive to spasm induction under conditions of sex hormone withdrawal.

5. Augmentation of arteriogenesis by angiogenic cytokines

Cytokines (Erythropoietin, G-CSF) were observed to enhance collateral formation from intact arteries in infarcted rat hearts. Collateral formation (equivalent to arteriogenesis) consists of arterioles ranging from 50 to 400 μm in diameter. Since conventional X-ray angiography cannot be used to identify vessels of less than 200 μm in diameter, only SR-MA is able to identify entire figures of arteriogenesis. This advantage of SR-MA may enable the future evaluation of vascular regeneration therapy both for ischemic heart disease and peripheral vascular disease.

S. Matsushita[1], K. Hyodo[2], S. Akishima[1], F. Sato[1], T. Imazuru[1], C. Tokunaga[1], Y. Enomoto[1], Y. Hiramatsu[1] and Y. Sakakibara[1] ([1]Univ. of Tsukuba, [2]KEK-PF)

References

[1] S. Akishima, S. Matsushita, F. Sato, K. Hyodo, T. Imazuru, Y. Enomoto, M. Noma, Y. Hiramatsu, O. Shigeta and Y. Sakakibara, *Circ. J.*, **71** (2007) 418.
[2] S. Matsushita, K. Hyodo, S. Akishima, F. Sato, T. Imazuru, M. Noma, Y. Hiramatsu, O. Shigeta and Y. Sakakibara, *Nucl. Instrum. Meth. Phys. Res. A*, **548** (2005) 94.

8-3 X-Ray Phase Imaging of Biological Soft Tissue Using a Direct-Sensing X-Ray HARP Tube Camera

X-ray phase-imaging is a powerful technique for observing biological soft tissues and organic materials because it offers two to three orders of magnitude higher sensitivity to light elements ($Z < 17$) than conventional absorption-contrast X-ray imaging. One of the most promising approaches for enhancing the sensitivity of X-ray phase-imaging is the use of a high-sensitivity X-ray camera equipped with a high-gain avalanche rushing amorphous photoconductor (HARP). At the Photon Factory several types of X-ray HARP cameras have been developed in collaboration with the NHK Science & Technical Research Laboratory (NHK-STRL) and NHK Engineering Service (NHK-ES). For example,

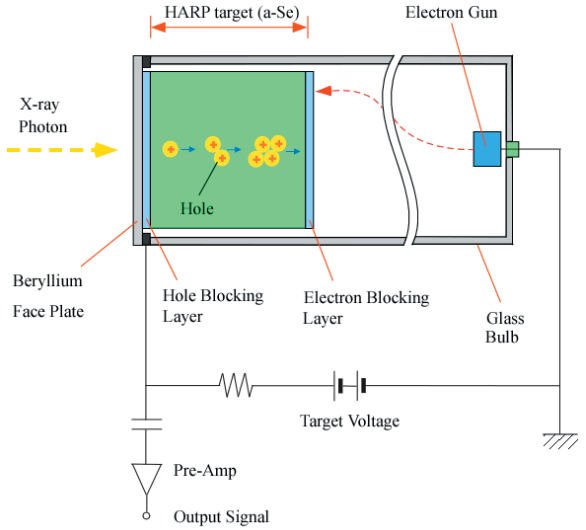

Figure 5
Schematic diagram of the direct-sensing X-ray HARP tube camera.

a diagram of a direct-sensing X-ray HARP tube camera is shown in Fig. 5. The diagonal length of the image area is 11 mm (2/3 inch type). Incoming X-ray photons are directly converted into electron-hole pairs in a 15 μm thick amorphous selenium (a-Se) photoconductor target. When a very high field (E > 80 V μm^{-1}) is applied to the a-Se layer, drifting holes can gain enough energy to generate further electron-hole pairs by impact ionization, and avalanche multiplication results in drastically enhanced sensitivity. The operation of the camera complies with the high definition television (HDTV) standard, and images are stored in real-time on a workstation at a rate of 30 images/s with an image format of 960 (H) × 1100 (V) pixels. The pixel size is 15.4 μm (H) × 8.1 μm (V), and the field of view is 15 mm (H) × 9 mm (V).

The first application of the X-ray HARP tube camera to X-ray phase imaging was carried out at BL-14B [1], using an experimental setup shown schematically in Fig. 6(a). A monochromatic X-ray beam (λ = 0.0766 nm) was incident on a triple Laue-case X-ray interferometer consisting of three parallel, equally-spaced crystal wafers (*S*, *M* and *A*). The beam is split into two when the incident X-rays satisfy the Bragg diffraction condition. Thus, the crystal wafers function as X-ray half mirrors, and two coherent beam paths are formed in the interferometer. A sample was cut from a rat liver fixed in formalin, and inserted in a cell filled with water for observation in a wet environment. The cell was placed in one of the beam paths of the interferometer. A plastic phase shifter, 0.4 mm in thickness, was placed in the other beam path for phase-map measurements. The X-ray HARP tube camera was used to observe the interference patterns produced by the sample. A voltage of 1300 V was applied to the HARP target to give an output signal gain of 2. The obtained phase map of the rat liver is shown in Fig. 6(b), where the phase shift ranges from 50° to 200°. Remarkably, blood vessel trees in the rat liver are clearly seen even without the use of a contrast agent. From the size of the blood vessels, the spatial resolution of the X-ray HARP tube camera was estimated to be better than 35 μm in the vertical direction and 100 μm in the horizontal direction. This result indicates that direct-sensing X-ray HARP tube cameras are useful for acquiring X-ray phase maps, *i.e.* for X-ray phase imaging. It would be possible to drastically reduce radiation exposure and/or measurement time by applying a higher voltage to the HARP target.

Experiments using animal samples were approved by the Medical Committee for the use of animals in research of the University of Tsukuba and KEK.

K. Hirano[1], T. Miyoshi[1], N. Igarashi[1], T. Takeda[2], J. Wu[2], T. T. Lwin[2], M. Kubota[3], N. Egami[3], K. Tanioka[3], T. Kawai[4] and S. Wakatsuki[1] ([1]KEK-PF, [2]Tsukuba Univ., [3]NHK, [4]NHK-ES)

Reference

[1] K. Hirano, T. Miyoshi, N. Igarashi, T. Takeda, J. Wu, T.T. Lwin, M. Kubota, N. Egami, K. Tanioka, T. Kawai and S. Wakatsuki, *Phys. Med. Biol.*, **52** (2007) 2545.

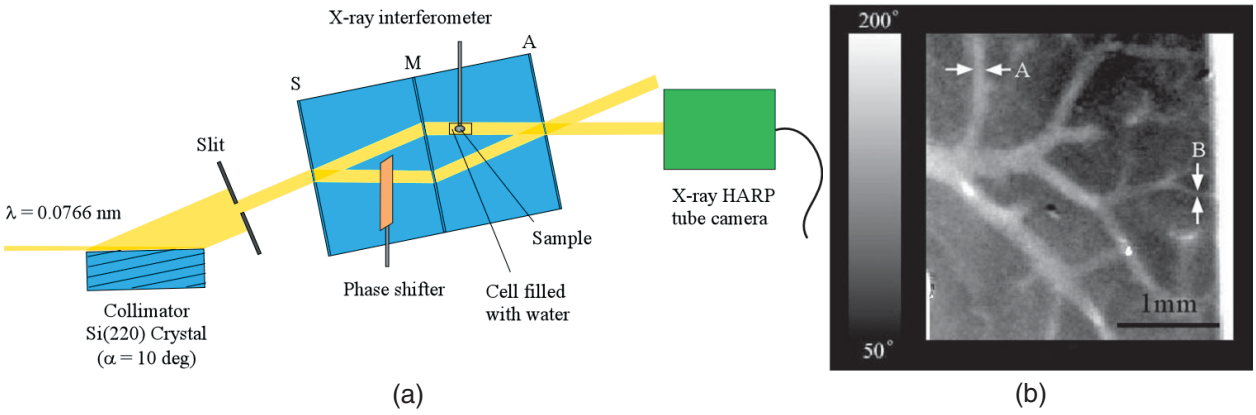

Figure 6
(a) The experimental setup for X-ray phase-imaging using an X-ray interferometer and the X-ray HARP camera. (b) Observed phase-map of rat liver.